Hindawi
Mathematical Problems in Engineering
Volume 2023, Article ID 6974834, 13 pages
https://doi.org/10.1155/2023/6974834

Research Article

Error Calibration of Cross Magnetic Gradient Tensor System with Total Least-Squares Method

Cheng Chi, Dan Wang, Ronghua Tao, and Zhentao Yu

Navy Submarine Academy, Qingdao 266001, China

Correspondence should be addressed to Cheng Chi; cheng.chihhu@163.com and Dan Wang; 13869887280@163.com

Received 10 October 2022; Revised 4 December 2022; Accepted 15 December 2022; Published 4 January 2023

Academic Editor: Hamid M. Sedighi

The magnetic gradient tensor system configured by fluxgate magnetometers is subjected to different scale factors, three-axis nonorthogonality, bias, and misalignment errors. All those errors above will influence the measurement precision directly, so the magnetic gradient tensor system must be calibrated before use. In this paper, an error calibration method of the magnetic gradient tensor system is proposed. The procedure of the proposed method is as follows. Firstly, the error calibration model of the single fluxgate magnetometer is established and generated an ellipsoid mathematical expression. To simplify the calculation, the ellipsoid mathematical expression is transformed into a linear model of intermediate variables, and then, error parameters are estimated by the total least-squares method. Secondly, the orthogonal procrustes problem is adopted to calibrate misalignment errors. Finally, simulations and experiments with a cross magnetic gradient tensor system are carried out for verification of the proposed error calibration method. Results show that compared with the original least-squares method, the proposed method can increase the measurement accuracy of the cross magnetic gradient tensor system greatly.

1. Introduction

Magnetic gradient tensor measurements [1–3] have many theoretical advantages over conventional magnetic surveys (i.e., vector and total magnetic intensity measurements). For example, tensor elements are true potential fields with desirable mathematical properties, magnetic gradient tensor measurements are relatively insensitive to orientation errors and geomagnetic gradients, and gradient tensor elements can provide valuable additional information and have better resolution. Based on those merits, magnetic gradient tensor measurements are widely used in magnetic target detection, demining, geological survey, and navigation. Over the past decades, there has been growing interest in developing magnetic gradient tensor systems, such as the hexahedron magnetic gradient tensor system designed by the Naval Surface Warfare Center [4] and the tetrahedron magnetic gradient tensor system designed by the DSO National Laboratories [5, 6].

Generally, superconducting quantum interference devices (SQUID) [7] or fluxgate magnetometers are two major sensors to construct a magnetic gradient tensor system. SQUID sensors have the merits of high sensitivity and precision, but the SQUID system needs to be liquid He-cooled or liquid nitrogen-cooled, which results in the SQUID system being complicated and expensive. Compared with SQUID sensors, fluxgate magnetometers have the advantages of small size, low power with relatively high sensitivity, and low cost [8], so there are many kinds of magnetic gradient tensor systems configured by fluxgate magnetometers. However, being restricted by technological limitations and manufacturing crafts, the magnetic gradient tensor system is subjected to different scale factors, three-axis nonorthogonality, bias, and misalignment errors [9]. All those errors above will influence the measurement precision directly, so the magnetic gradient tensor system must be calibrated before use.

Magnetic gradient tensor system is always configured by several vector magnetometers, so the error calibration process can be divided into two steps: the first step is to calibrate the single vector magnetometer, and the second step is to calibrate misalignment errors between

magnetometers. Many research papers have a focus on the calibration of single vector magnetometer, and the calibration method can be divided into vector calibration and scalar calibration.

Vector calibration [10, 11] needs a rigorous calibration magnetic field and a high-precision tri-axial nonmagnetic platform, the calibration equipment is very expensive, and the calibration procedure is complicated, so vector calibration is not suitable for practical applications. However, on the other hand, scalar calibration [12–14] is usually described as the "poor man's" calibration method, because scalar calibration only needs a high-precision proton magnetometer to monitor the background geomagnetic field, and the calibration procedure is simple and easy to perform. Yu et al. [12, 13] proposed a calibration method for a magnetic vector gradiometer, but two or higher-order small quantities were omitted in this method, and the precision of the corrected outs was reduced. Gang et al. [14] calibrated the magnetic gradient tensor system using a linear calibration method, but two nonlinear conversions were used to linearize the nonlinear mathematical model of single vector magnetometer calibration, and the calculation process was complicated. Zhen-tao et al. [15] achieved calibration of the tetrahedron magnetic gradiometer with the restriction of traceless and symmetric properties. Calibration matrixes were estimated with a genetic algorithm; however, the optimization algorithm was easily trapped into local optimization, and the convergent speed was slow.

In this paper, an error calibration method of the cross magnetic gradient tensor system is proposed, and the calibration process is divided into two steps. Firstly, considering the scale factors, bias, and three-axis nonorthogonal errors, an error calibration model of the single fluxgate magnetometer is established, the nonlinear calibration model is transformed into a linear model of intermediate variables, and least-squares approximation method is a traditional method to solve an over-determined system of equations, which is called the original method in this paper; however, the least-squares method is asymmetry, and motivated by this, the total least-squares method is introduced to calculate the error parameters in this paper, which is called the proposed method. Secondly, the orthogonal procrustes problem is adopted to calibrate misalignment errors. Simulations and experiments are carried out, and the results show that the proposed error calibration method can improve the measurement accuracy of the cross magnetic gradient tensor system.

2. The Configuration and Error Model of Cross Magnetic Gradient Tensor System

2.1. The Configuration of Cross Magnetic Gradient Tensor System. The magnetic gradient tensor is defined as the vector gradient of the magnetic flux density in three orthogonal directions, and the magnetic gradient tensor can be represented by the following 3×3 matrix:

$$\begin{aligned}\mathbf{G} &= \nabla \mathbf{B} \\ &= \begin{bmatrix} \frac{\partial B_x}{\partial x} & \frac{\partial B_x}{\partial y} & \frac{\partial B_x}{\partial z} \\ \frac{\partial B_y}{\partial x} & \frac{\partial B_y}{\partial y} & \frac{\partial B_y}{\partial z} \\ \frac{\partial B_z}{\partial x} & \frac{\partial B_z}{\partial y} & \frac{\partial B_z}{\partial z} \end{bmatrix} \\ &= \begin{bmatrix} G_{11} & G_{12} & G_{13} \\ G_{21} & G_{22} & G_{23} \\ G_{31} & G_{32} & G_{33} \end{bmatrix}.\end{aligned} \tag{1}$$

There are nine components in the matrix **G**. In an area that does not contain conduction currents, both the divergence and the curl of the magnetic flux density are zero, so the tensor is traceless and symmetric [16].

$$\begin{cases} \nabla \cdot \mathbf{B} = \dfrac{\partial B_x}{\partial x} + \dfrac{\partial B_y}{\partial y} + \dfrac{\partial B_z}{\partial z} = 0, \\ \nabla \times \mathbf{B} = \begin{vmatrix} i & j & k \\ \frac{\partial}{\partial x} & \frac{\partial}{\partial y} & \frac{\partial}{\partial z} \\ B_x & B_y & B_z \end{vmatrix} = 0. \end{cases} \tag{2}$$

According to equations (1) and (2), the number of independent components is reduced to 5, so the magnetic gradient tensor matrix can be obtained by measuring the independent 5 components.

The magnetic gradient tensor components cannot be measured intrinsically in an actual measurement application, so the tensor components are approximated by the difference between two measurement readings of the magnetic field at different locations. However, the real measured value is slightly different compared to the theoretical value, and this difference is commonly called structure error. Structure error is usually affected by different configurations of fluxgate magnetometers. The structure error of different configurations is analyzed in reference [17], and research results show that the cross magnetic gradient tensor system has minimal structure error. Based on the above results, a cross magnetic gradient tensor system is designed in this paper, and the configuration of the cross magnetic gradient tensor system is shown in Figure 1.

As shown in Figure 1, a right-handed coordinate system is established, and the cross magnetic gradient tensor system comprises four fluxgate magnetometers (1 to 4). Four magnetometers lie on the plane xoy, and the baseline

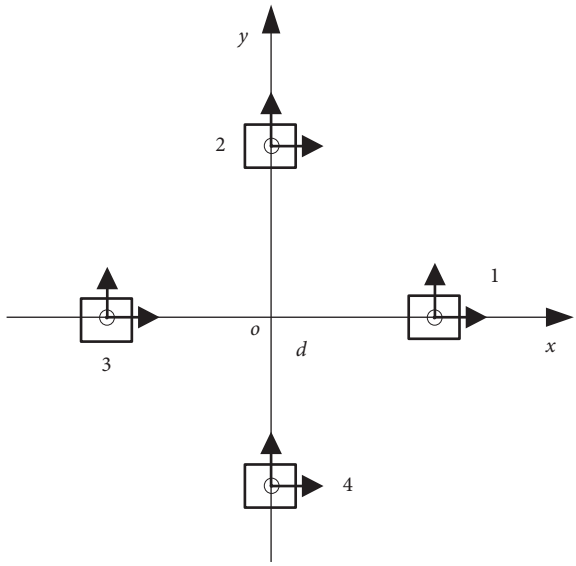

Figure 1: The configuration of the cross magnetic gradient tensor system.

distance between two magnetometers along the same axes is d. The magnetic gradient tensor of the point o can be estimated by the measurement readings of four fluxgate magnetometers:

$$\mathbf{G} = \frac{1}{d}\begin{bmatrix} B_{1x} - B_{3x} & B_{2x} - B_{4x} & B_{1z} - B_{3z} \\ B_{1y} - B_{3y} & B_{2y} - B_{4y} & B_{2z} - B_{4z} \\ B_{1z} - B_{3z} & B_{2z} - B_{4z} & B_{4y} - B_{2y} + B_{3x} - B_{1x} \end{bmatrix}, \quad (3)$$

where B_{ij} $(i = 1, 2, 3, 4,\ j = x, y, z)$ is the j component of the magnetometer i.

2.2. Error Calibration Model for Single Fluxgate Magnetometer. Due to manufacturing imperfections, the fluxgate magnetometer is subjected to nonorthogonal error, different scale factors, and bias. Nonorthogonal error is that the three actual axes of the fluxgate magnetometer may not coincide with the three-orthogonal axis. The geometrical relationship of the nonorthogonal angles is shown in Figure 2, suppose $O - XYZ$ is the actual measurement coordinate system of the fluxgate magnetometer, $O - X_0Y_0Z_0$ is an ideal three-axis orthogonal coordinate system, and suppose the measurement axis OZ is completely aligned with the ideal coordinate axis OZ_0. The plane YOZ is coplanar with the plane Y_0OZ_0. The angle between the axis OY and OY_0 is ψ. OX' is the projection of the measurement axis OX in the plane X_0OY_0, the angle between the axis OX and OX' is θ, and the angle between the axis OX_0 and OX' is φ.

Each measurement axis of the fluxgate magnetometer has different biases and sensitivities, so we define $\mathbf{b} = [b_x, b_y, b_z]^{\mathrm{T}}$ as the biases and k_x, k_y, k_z as the scale factors (sensitivities) for OX, OY, OZ axes. Suppose $\mathbf{B}$ are the theoretical outputs under the ideal three-axis orthogonal coordinate system $O - X_0Y_0Z_0$, $\mathbf{B}_m$ are the actual outputs of the fluxgate magnetometer, and

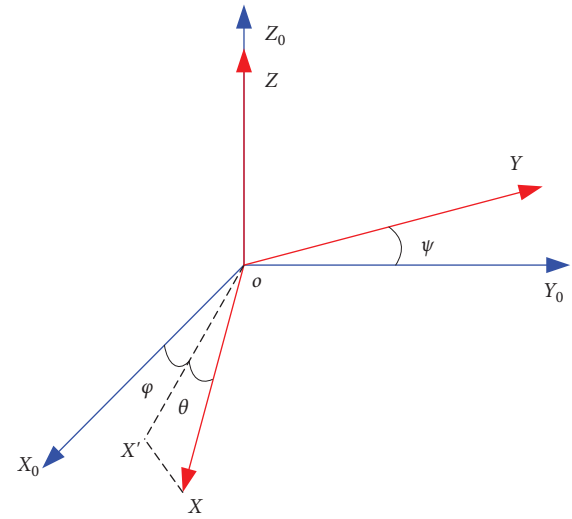

Figure 2: Geometrical relationship of the nonorthogonal angles.

then, the relationship between $\mathbf{B}_m$ and $\mathbf{B}$ can be written as follows:

$$\begin{aligned}\mathbf{B}_m &= \begin{bmatrix} k_x & 0 & 0 \\ 0 & k_y & 0 \\ 0 & 0 & k_z \end{bmatrix}\begin{bmatrix} \cos\theta\cos\varphi & \cos\theta\sin\varphi & \sin\theta \\ 0 & \cos\psi & \sin\psi \\ 0 & 0 & 1 \end{bmatrix}\mathbf{B} + \mathbf{b} + \boldsymbol{\varepsilon} \\ &= \mathbf{S}\mathbf{C}_{NO}\mathbf{B} + \mathbf{b} + \boldsymbol{\varepsilon},\end{aligned} \quad (4)$$

where $\mathbf{S}$ is the scale factor matrix, $\mathbf{C}_{NO}$ is the nonorthogonal error coefficient matrix, and ε is the measurement noise of the magnetometer. Equation (4) is the error model of the fluxgate magnetometer.

Define the combined error parameter matrix $\mathbf{C} = \mathbf{S}\mathbf{C}_{NO}(\mathbf{I} + \mathbf{K})$, and then, the error model of the fluxgate magnetometer can be described by

$$\mathbf{B}_m = \mathbf{C}\mathbf{B} + \mathbf{b} + \boldsymbol{\varepsilon}. \quad (5)$$

Compared with the nonorthogonal error, different scale factors, and bias, the measurement noise is relatively small, and hence, it is negligible, and then, the error calibration model for the fluxgate magnetometer can be written as follows:

$$\mathbf{B} = \mathbf{C}^{-1}(\mathbf{B}_m - \mathbf{b}). \quad (6)$$

According to equation (6), we know that the error calibration for a single fluxgate magnetometer is to estimate the calibration matrices $\mathbf{C}$ and $\mathbf{b}$, and then, the corrected output $\mathbf{B}$ can be obtained by equation (6).

2.3. Misalignment Error Model. Due to technical limitations, the four fluxgate magnetometers cannot be completely aligned with each other, and then, the misalignment error is brought out. We calibrate the misalignment error using one of the sensors as a reference. We use magnetometer 1 as a reference, and the actual outputs of magnetometer 2–4 are transformed into the reference orthogonal coordinate system of magnetometer 1. As shown in Figure 3, $OX_1Y_1Z_1$ is the reference

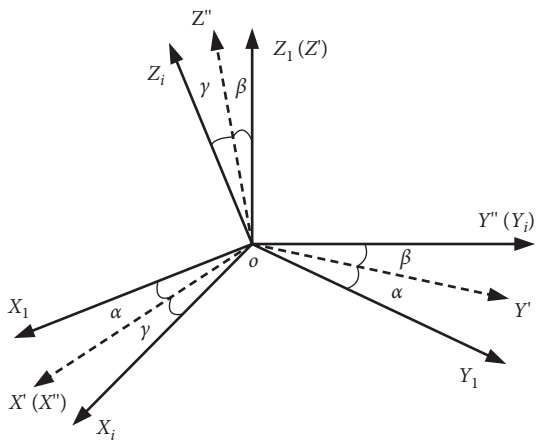

Figure 3: Misalignment angles of the magnetometer i.

orthogonal coordinate system, and $OX_iY_iZ_i$ is the orthogonal coordinate system of the magnetometer i. $OX_1Y_1Z_1$ can be converted to $OX_iY_iZ_i$ by rotating around three orthogonal axes. As shown in Figure 3, the procedure is as follows: firstly, rotate $OX_1Y_1Z_1$ through angle α about Z_1 axes to $OX'Y'Z'$, then rotate $OX'Y'Z'$ through angle β about X' axes to $OX''Y''Z''$, and at last, rotate $OX''Y''Z''$ through angle γ about Y'' axes to $OX_iY_iZ_i$. α, β, γ are misalignment angles.

The mathematical relationship between the output of the magnetometer i and the output of the reference magnetometer is described as follows:

$$\mathbf{B}_i = \mathbf{R}_1\mathbf{R}_2\mathbf{R}_3\mathbf{B}_1, \tag{7}$$

where $\mathbf{R}_1 = \begin{bmatrix} \cos\gamma & 0 & -\sin\gamma \\ 0 & 1 & 0 \\ \sin\gamma & 0 & \cos\gamma \end{bmatrix}$, $\mathbf{R}_2 = \begin{bmatrix} 1 & 0 & 0 \\ 0 & \cos\beta & \sin\beta \\ 0 & -\sin\beta & \cos\beta \end{bmatrix}$, and $\mathbf{R}_3 = \begin{bmatrix} \cos\alpha & \sin\alpha & 0 \\ -\sin\alpha & \cos\alpha & 0 \\ 0 & 0 & 1 \end{bmatrix}$ are three coordinate-transformation matrices. Equation (7) is the misalignment error model of the magnetometer i, and once the coordinate-transformation matrices are obtained, the actual outputs of the magnetometer i can be transformed into the reference orthogonal coordinate system.

As discussed in Section 2.1, the tensor components are estimated using the difference between two measurement values of the magnetic field at different locations. Nonorthogonal error, different scale factors, bias, and misalignment errors of the magnetometers will influence the measurement precision directly, so the magnetic gradient tensor system must be calibrated before use.

3. Error Calibration of Cross Magnetic Gradient Tensor System

3.1. Error Calibration of Single Fluxgate Magnetometer. Within a homogeneous magnetic field, the intensity of the magnetic field is constant. By multiplying both sides of equation (6) with the transpose, we can obtain

$$\begin{aligned} \mathbf{B}^{\mathrm{T}}\mathbf{B} &= (\mathbf{B}_m - \mathbf{b}_o)^{\mathrm{T}}(\mathbf{C})^{\mathrm{T}}\mathbf{C}(\mathbf{B}_m - \mathbf{b}_o) \\ &= \text{const.} \end{aligned} \tag{8}$$

Define $\mathbf{A} = (\mathbf{C}^{-1})^{\mathrm{T}}\mathbf{C}^{-1}$, and the following equation is obtained:

$$\mathbf{B}_m^{\mathrm{T}}\mathbf{A}\mathbf{B}_m - 2\mathbf{b}^{\mathrm{T}}\mathbf{A}\mathbf{B}_m + \mathbf{b}^{\mathrm{T}}\mathbf{A}\mathbf{b} - \mathbf{B}^{\mathrm{T}}\mathbf{B} = 0. \tag{9}$$

Equation (9) is the expression of an ellipsoidal surface. Within a homogeneous magnetic field, the distribution surface of actual outputs is an ellipsoidal surface, and the distribution surface of theoretical outputs is a standard sphere, so the error calibration of the fluxgate magnetometer is a problem of the ellipsoidal surface fitting. Suppose the actual output of the fluxgate magnetometer is $[x, y, z]^{\mathrm{T}}$, the general mathematical expression of an ellipsoid can be written as follows:

$$\begin{aligned} ax^2 + by^2 + cz^2 + 2fyz + 2gxz + 2hxy \\ + 2px + 2qy + 2rz + d = 0. \end{aligned} \tag{10}$$

Both sides of equation (10) are divided by the parameter p, and the following equation is obtained:

$$\frac{a}{p}x^2 + \frac{b}{p}y^2 + \frac{c}{p}z^2 + 2\frac{f}{p}yz + 2\frac{g}{p}xz + 2\frac{h}{p}xy + 2\frac{q}{p}y + 2\frac{r}{p}z + \frac{d}{p} = -2x. \tag{11}$$

A set of actual outputs $\left\{[x_i, y_i, z_i]^{\mathrm{T}}\right\}_{i=1}^{N}$ is obtained by presenting the magnetometer in different orientations. Best estimates for parameters $(a/p, b/p, c/p, f/p, g/p, h/p, q/p, r/p, d/p)$ in the least-squares sense can be found by restructuring equation (11) because the parameters are constant for all N measurements.

$$\mathbf{X}_{N\times 9}\mathbf{P}_{9\times 1} = \mathbf{W}_{N\times 1}, \tag{12}$$

where $\mathbf{P} = 1/p\left[\begin{array}{ccccccccc} a & b & c & f & g & h & q & r & d \end{array}\right]^{\mathrm{T}}$, $\mathbf{W} = \left[\begin{array}{cccc} -2x_1 & -2x_2 & \cdots & -2x_N \end{array}\right]^{\mathrm{T}}$, $\mathbf{X} = \begin{bmatrix} x_1^2 & y_1^2 & z_1^2 & 2y_1z_1 & 2x_1z_1 & 2x_1y_1 & 2y_1 & 2z_1 & 1 \\ x_2^2 & y_2^2 & z_2^2 & 2y_2z_2 & 2x_2z_2 & 2x_2y_2 & 2y_2 & 2z_2 & 1 \\ \vdots & \vdots & \vdots & \vdots & \vdots & \vdots & \vdots & \vdots & \vdots \\ x_N^2 & y_N^2 & z_N^2 & 2y_Nz_N & 2x_Nz_N & 2x_Ny_N & 2y_N & 2z_N & 1 \end{bmatrix}$. Since $\mathrm{rank}(\mathbf{X}) = 9 \le N$, equation (12) has no exact solution. Finally, the least-squares approximation for the parameter matrix $\widehat{\mathbf{P}}$ can be obtained by

$$\widehat{\mathbf{P}}_{\mathrm{LS}} = \left(\mathbf{X}\mathbf{X}^{\mathrm{T}}\right)^{-1}\mathbf{X}\mathbf{W}. \tag{13}$$

The matrix $\mathbf{W}$ is affected by the magnetic noise, and the least-squares approximation is obtained as a solution to the optimization problem [18–20].

$$\begin{aligned} &\left\{\widehat{\mathbf{P}}_{\mathrm{LS}}, \Delta\mathbf{W}_{\mathrm{TLS}}\right\} := \arg\min_{\mathbf{P},\Delta\mathbf{W}} \|\Delta\mathbf{W}\|_F \\ &\text{subject to } \mathbf{X}\mathbf{P} = \mathbf{W} + \Delta\mathbf{W}. \end{aligned} \tag{14}$$

However, both $\mathbf{X}$ and $\mathbf{W}$ are measurement data, and the matrix $\mathbf{X}$ is also affected by the magnetic noise. From equation (14), $\mathbf{W}$ is corrected while $\mathbf{X}$ is not, and then, the

least-squares method is asymmetry. Provided that both $\mathbf{X}$ and $\mathbf{W}$ are affected by the magnetic noise, it is reasonable to treat them symmetrically, and then, the optimization problem becomes that

$$\left\{\widehat{\mathbf{P}}_{\mathrm{TLS}}, \Delta\mathbf{X}_{\mathrm{TLS}}, \Delta\mathbf{W}_{\mathrm{TLS}}\right\} := \arg\min_{\mathbf{P},\Delta\mathbf{X},\Delta\mathbf{W}} \left\| [\,\Delta\mathbf{X} \;\; \Delta\mathbf{W}\,] \right\|_F \quad \text{subject to } (\mathbf{X}+\Delta\mathbf{X})\mathbf{P} = \mathbf{W}+\Delta\mathbf{W}. \tag{15}$$

The estimated solution of equation (15) can be obtained by the total least-squares method [21, 22]. Define the matrix $\mathbf{G} = [\,\mathbf{X} \;\; \mathbf{W}\,]$, and the singular value decomposition of the matrix $\mathbf{G}$ is written as follows:

$$\mathbf{C} = [\,\mathbf{X} \;\; \mathbf{W}\,] = \mathbf{U}\sum\mathbf{V}^{\mathrm{T}}, \text{where } \Sigma = \mathrm{di\,ag}(\sigma_1, \sigma_2, \ldots, \sigma_{10}), \tag{16}$$

where $\sigma_1, \sigma_2, \ldots, \sigma_{10}$ are the singular values of the matrix $\mathbf{C}$, and the right unitary matrix $\mathbf{V}$ can be rewritten as follows:

$$\mathbf{V}_{10\times10} = \begin{matrix} \\ 9 \\ 1 \end{matrix} \begin{matrix} \begin{matrix} 9 & 1 \end{matrix} \\ \begin{bmatrix} \mathbf{V}_{11} & \mathbf{V}_{12} \\ \mathbf{V}_{21} & \mathbf{V}_{22} \end{bmatrix} \end{matrix} \tag{17}$$

If $\mathbf{V}_{22}$ is nonsingular, then the total least-squares solution exists and is given by

$$\widehat{\mathbf{P}}_{\mathrm{TLS}} = -\mathbf{V}_{12}\mathbf{V}_{22}^{-1}. \tag{18}$$

$\widehat{\mathbf{P}}_{\mathrm{TLS}}$ is a total least-squares solution of equation (12). The relationship between the calibration matrices $\mathbf{A}, \mathbf{b}$ and the estimated error parameters is as follows:

$$\mathbf{A} = \begin{bmatrix} \widehat{a} & \widehat{h} & \widehat{g} \\ \widehat{h} & \widehat{b} & \widehat{f} \\ \widehat{g} & \widehat{f} & \widehat{c} \end{bmatrix}, \tag{19}$$

$$\mathbf{b} = -\mathbf{A}^{-1}\begin{bmatrix} \widehat{p} \\ \widehat{q} \\ \widehat{r} \end{bmatrix}, \tag{20}$$

$$\mathbf{b}^{\mathrm{T}}\mathbf{A}\mathbf{b} - \mathbf{B}^{\mathrm{T}}\mathbf{B} = \widehat{d}. \tag{21}$$

The measurement is carried out within a homogeneous magnetic field, and the intensity of the magnetic field $\|\mathbf{B}\|$ is measured by a scalar proton magnetometer. The calibration matrices $\mathbf{A}, \mathbf{b}$ can be obtained by solving equations (19)–(21). Thus, to accomplish the calibration of the single magnetometer, we need to estimate the parameter matrix $\mathbf{C}^{-1}$. Since $\mathbf{A}$ is a symmetric positive definite matrix, the Cholesky factorization [19] of $\mathbf{A}$ provides a unique upper triangular matrix $\mathbf{C}^{-1}$, such that $(\mathbf{C}^{-1})^{\mathrm{T}}\mathbf{C}^{-1} = \mathbf{A}$. Then, the calibrated output $\mathbf{B}$ of a single magnetometer can be obtained by equation (6).

3.2. Misalignment Error Calibration. According to the misalignment error model of the magnetometer i (2–4), the misalignment error calibration of the magnetometer i (2–4) is to estimate the coordinate-transformation matrices, and the orthogonal procrustes problem [23] is adopted to determine the coordinate-transformation matrices in this paper.

Suppose we get $N\,(N \geq 3)$ groups of measurement data by presenting the cross magnetic gradient tensor system in different attitudes. After the error calibration for a single fluxgate magnetometer, the corrected outputs of magnetometer i are $\mathbf{M}_i = [\mathbf{B}_{i1} \cdots \mathbf{B}_{iN}]$, where $\mathbf{B}_{iN} = [B_{iNx}, B_{iNy}, B_{iNz}]^{\mathrm{T}}$, the corrected outputs of the reference magnetometer are $\mathbf{M}_1 = [\mathbf{B}_{11} \cdots \mathbf{B}_{1N}]$, suppose $\mathbf{M}_1\mathbf{M}_i^{\mathrm{T}}$ is nonsingular, the singular value decomposition of the matrix $\mathbf{M}_1\mathbf{M}_i^{\mathrm{T}}$ is $\mathbf{M}_1\mathbf{M}_i^{\mathrm{T}} = \mathbf{U}_M\sum\mathbf{V}_M^{\mathrm{T}}$, where $\mathbf{U}_M, \mathbf{V}_M$ are 3×3 unitary matrices, and Σ is a diagonal matrix. The optimal orthogonal matrix $\mathbf{R}$ minimizes the transformation from $\mathbf{M}_i$ to $\mathbf{M}_1$, specifically,

$$\min_{\mathbf{R}} \sum_{j=1}^{N} \left\| \mathbf{B}_{1j} - \mathbf{R}\mathbf{B}_{ij} \right\|^2 \text{ subject to } \mathbf{R}^{\mathrm{T}}\mathbf{R} = \mathbf{I}. \tag{22}$$

The optimal solution of equation (22) is unique and given by $\mathbf{R} = \mathbf{U}_M\mathbf{V}_M^{\mathrm{T}}$, and then, the corrected outputs of magnetometer i can be transformed into the reference orthogonal coordinate system.

4. Simulations and Experiments

4.1. Simulations. Simulations are performed to verify the performance of the proposed calibration method with Matlab. We set the average total intensity of the geomagnetic field as 50000 nT, the declination angle as -7°, and the inclination angle as 55°. Four simulative magnetometers are used to configure the simulated cross magnetic gradient tensor system, the baseline distance is 0.5 m, and error parameters of the four simulative magnetometers are shown in Table 1. Put the cross magnetic gradient tensor system under the uniform geomagnetic field environment, and the sampling data are obtained by presenting the cross magnetic gradient tensor system in different orientations. 1000 groups of measurement data under different system orientations are recorded.

To simulate the magnetic noise of the measurement, we add independent Gaussian white noises with a mean of 0 nT and a variance of 6nT in each axis of the different magnetometers. With 1000 groups of measurement data, error calibration parameters are estimated by the total least-squares method, and error calibration matrices calculated by the proposed method are shown in Table 2. The raw data are calibrated using the error calibration matrices as shown in Table 2. To compare the calibration performance, the corrected outputs of the original calibration method and the proposed method are both shown in Figures 4 and 5.

According to the simulation results, the fluctuations of the magnetic field intensity and magnetic gradient tensor components are large before calibration, and the fluctuations are mainly caused by the measurement of the system under different orientations. After calibration, the fluctuations of the corrected outputs decrease obviously. As shown in Figure 4, before calibration, the max deviation of the

Table 1: Error parameters of the simulated cross magnetic gradient tensor system.

	Sensor 1	Sensor 2	Sensor 3	Sensor 4
k_x	1.045	1.053	1.065	0.973
k_y	0.981	1.041	0.985	1.033
k_z	0.975	0.971	1.049	1.042
b_x/nT	129	−83	85	93
b_y/nT	88	76	93	71
b_z/nT	−74	131	−65	−89
ψ/rad	0.051	0.026	−0.044	0.047
φ/rad	0.037	−0.033	0.035	0.042
θ/rad	−0.029	0.049	0.039	−0.031
α/rad	0	0.032	0.043	−0.035
β/rad	0	0.042	0.036	0.031
γ/rad	0	0.035	0.037	0.045

Table 2: Error calibration matrices of the proposed method.

	$\mathbf{C}^{-1}$	$\mathbf{b}$	$\mathbf{R}$
Sensor 1	$\begin{bmatrix} 0.958 & -0.0378 & 0.0317 \\ 0 & 1.0207 & -0.0524 \\ 0 & 0 & 1.0257 \end{bmatrix}$	$\begin{bmatrix} 129.374 \\ 86.4032 \\ -73.8938 \end{bmatrix}$	
Sensor 2	$\begin{bmatrix} 0.9514 & 0.0317 & -0.0514 \\ 0 & 0.961 & -0.0268 \\ 0 & 0 & 1.0299 \end{bmatrix}$	$\begin{bmatrix} -83.2236 \\ 76.9102 \\ 130.8063 \end{bmatrix}$	$\begin{bmatrix} 0.9988 & -0.032 & 0.0363 \\ 0.0334 & 0.9986 & -0.0408 \\ -0.035 & 0.042 & 0.9985 \end{bmatrix}$
Sensor 3	$\begin{bmatrix} 0.9403 & -0.0356 & -0.0387 \\ 0 & 1.0163 & 0.042 \\ 0 & 0 & 0.9533 \end{bmatrix}$	$\begin{bmatrix} 85.773 \\ 93.115 \\ -64.9406 \end{bmatrix}$	$\begin{bmatrix} 0.9983 & -0.043 & 0.0385 \\ 0.0443 & 0.9984 & -0.0343 \\ -0.037 & 0.036 & 0.9987 \end{bmatrix}$
Sensor 4	$\begin{bmatrix} 1.0292 & -0.0407 & 0.0317 \\ 0 & 0.9692 & -0.0451 \\ 0 & 0 & 0.9597 \end{bmatrix}$	$\begin{bmatrix} 93.3409 \\ 70.9987 \\ -88.8917 \end{bmatrix}$	$\begin{bmatrix} 0.9984 & 0.035 & 0.0439 \\ -0.0336 & 0.9989 & -0.0325 \\ -0.045 & 0.031 & 0.9985 \end{bmatrix}$

magnetic field intensity is 3916 nT; however, the max deviation of the corrected data is 14 nT.

As shown in Figure 5, before calibration, the max deviation of the tensor components is 12290 nT/m, and after calibration, the max deviation is reduced to 34.4 nT/m, so we can see that both the original calibration method and the proposed method can calibrate the magnetic gradient tensor system effectively.

RMS (root-mean-square) errors are used to represent the error calibration performance, and the formula is written as follows:

$$E_{\mathrm{RMS}} = \sqrt{\frac{1}{N}\sum_{i=1}^{N} e_i^2}, \tag{23}$$

where e_i is the calibration error between corrected data and ideal data, and N is the number of measurement orientations. Then, the RMS errors of total magnetic intensity before and after calibration are listed in Table 3. RMS errors of tensor components before and after calibration are listed in Table 4.

According to the RMS errors of total magnetic intensity shown in Table 3, the background geomagnetic intensity is uniform, and both the original calibration method and the proposed method can achieve the accurate calibration of the single magnetometer, so the RMS errors of corrected data are in the Gaussian noise error range; however, the performance of the original method is slightly worse. According to the RMS errors of tensor components before and after calibration shown in Table 4, RMS errors of all the components calibrated by the proposed method are smaller than the original method, and the RMS errors of B_{xy} can be reduced by 31.6% of errors of the original method.

4.2. Experiments. Experiments were carried out in Heikuang Mountain, Yantai, China, where the external magnetic interference was very low. A cross magnetic gradient tensor system consisting of four homemade fluxgate magnetometers is shown in Figure 6. To avoid additional magnetic interference, the holder is made of aluminum. The baseline distance of the system is 0.26 m. To find a relatively steady background geomagnetic field, a proton magnetometer is used, the accuracy of the proton magnetometer is 1 nT, and the resolution is 0.1 nT. The average value of the measured background geomagnetic intensity was 52368.3 nT. 80 groups of measurement data were recorded by presenting the cross magnetic gradient tensor system in different orientations. Then, we used the measurement data to calibrate the cross magnetic gradient tensor system, and the results were shown in Figures 7 and 8. As we knew that in a uniform

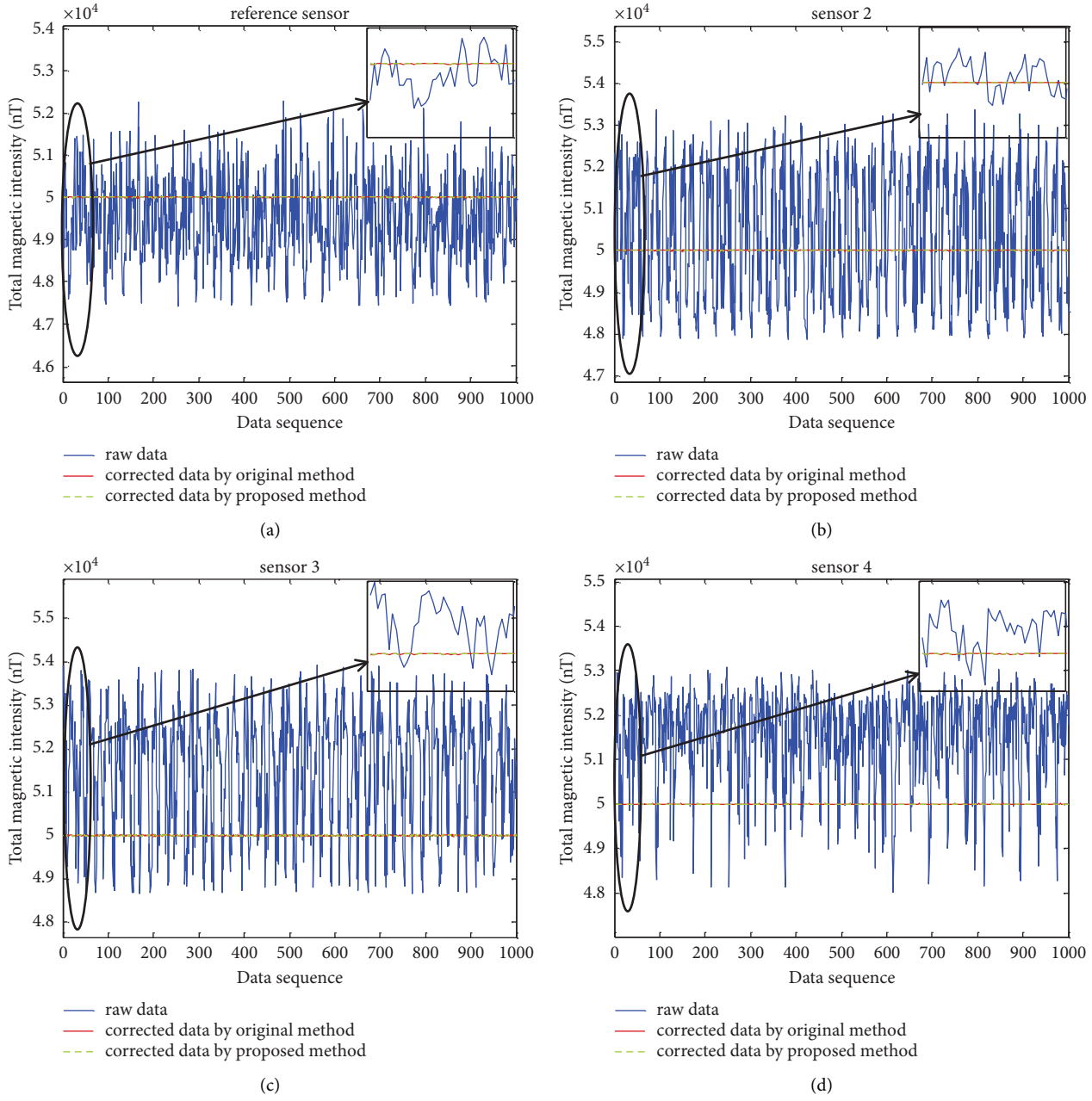

Figure 4: Comparison of total magnetic intensity before and after calibration.

geomagnetic field, the corrected output of the total magnetic intensity should be close to the background geomagnetic intensity, and the corrected output of the magnetic gradient tensor components should be close to 0 nT/m. As shown in Figure 7, the fluctuations of raw data are large, and the max fluctuation of the raw data is up to 3880 nT, and after calibration, fluctuation of total magnetic intensity is descended evidently, the corrected outputs are close to 52368.3 nT, the corresponding RMS errors of the four fluxgate magnetometers are presented in Table 5, and both the original method and the proposed method can calibrate the single fluxgate magnetometer's error effectively. As shown in Figure 8, because of the single fluxgate magnetometer errors and misalignment errors, the actual outputs of the magnetic gradient tensor components have big deviations, and after calibration, the corrected outputs are close to 0 nT/m. The corresponding RMS errors of tensor components are presented in Table 6, the RMS errors of the proposed method are smaller than the original method, and the RMSE of B_{xy} can be reduced to 31.316 nT/m by the original method; however, the RMSE of B_{xy} calibrated by the proposed method is 14.158 nT/m, and 54.79% of errors can be reduced by the proposed method, so the results of the experiments show

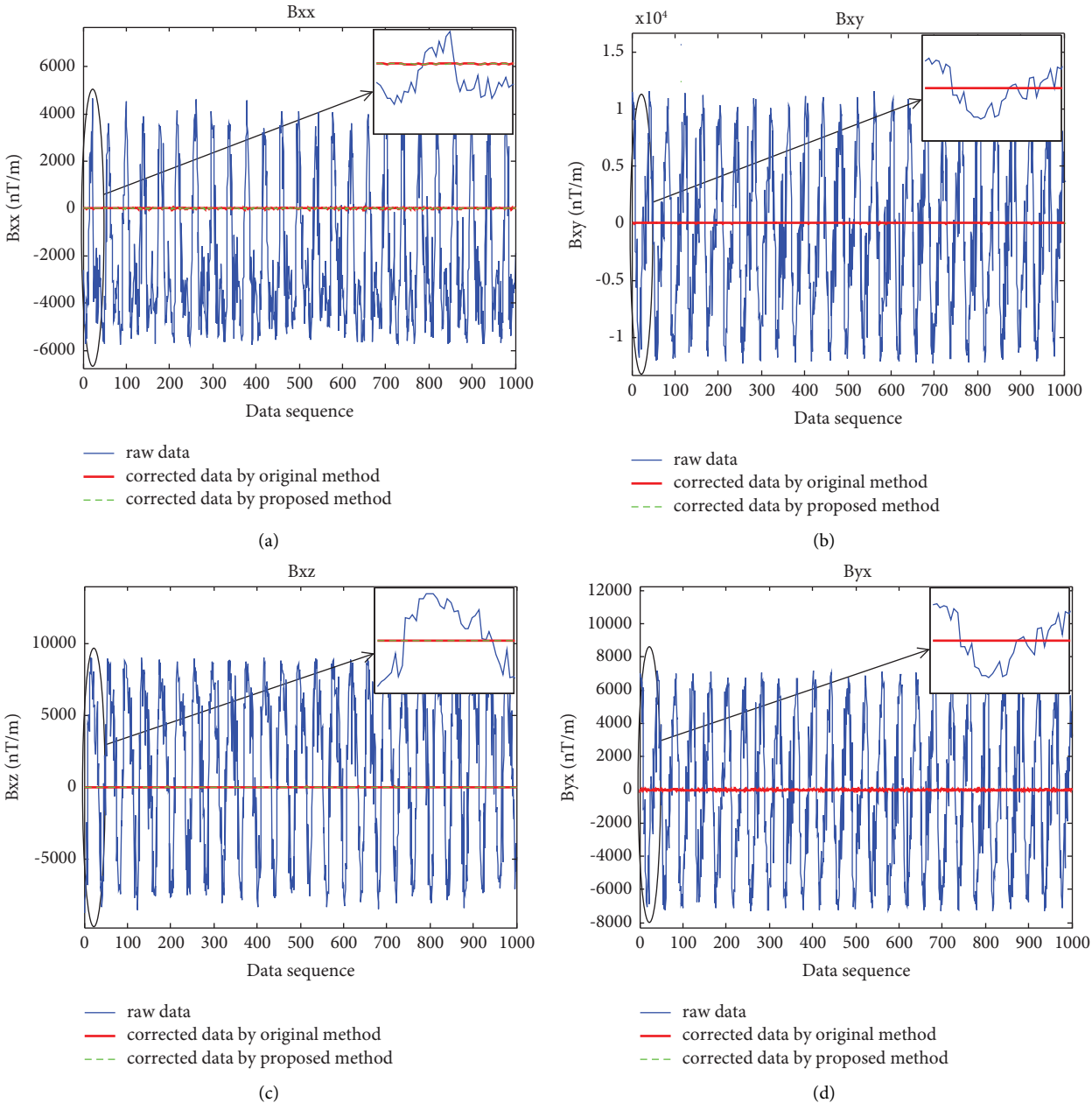

Figure 5: Continued.

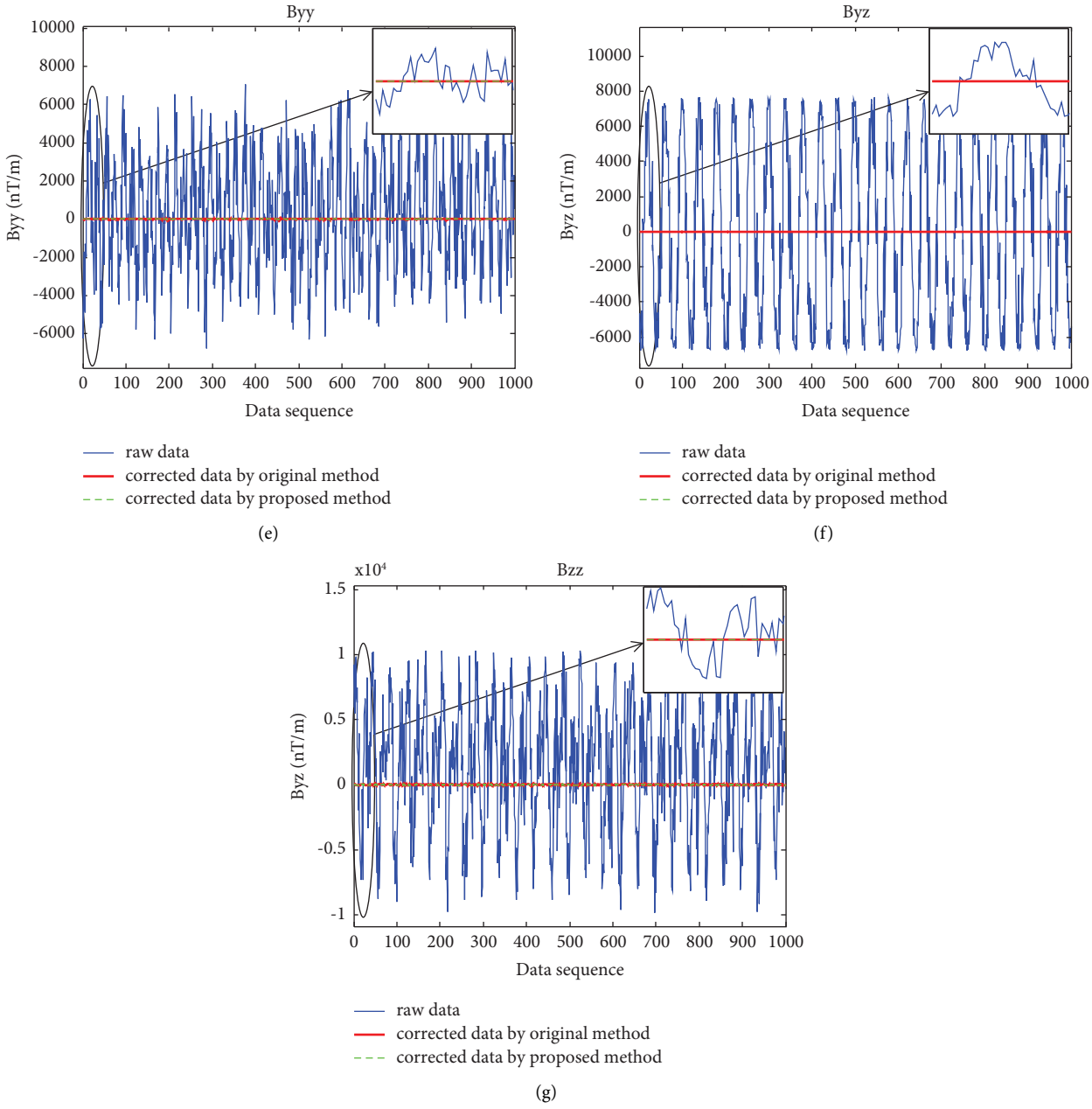

Figure 5: Comparison of tensor components before and after calibration.

Table 3: RMS errors of total magnetic intensity before and after calibration.

	Reference sensor (nT)	Sensor 2 (nT)	Sensor 3 (nT)	Sensor 4 (nT)
Raw data	1112.7	1576.1	2073.5	1799.8
Corrected data by the original method	3.914	4.037	3.873	4.035
Corrected data by the proposed method	3.892	3.989	3.829	3.993

Table 4: RMS errors of tensor components before and after calibration.

	B_{xx} (nT/m)	B_{xy} (nT/m)	B_{xz} (nT/m)	B_{yx} (nT/m)	B_{yy} (nT/m)	B_{yz} (nT/m)	B_{zz} (nT/m)
Raw data	3549.9	6958	5765.3	4455.6	2920.4	5036.6	5113.1
Corrected data by the original method	6.242	9.917	7.069	7.499	7.21	7.115	9.55
Corrected data by the proposed method	6.142	6.785	7.067	7.299	6.953	7.113	9.468

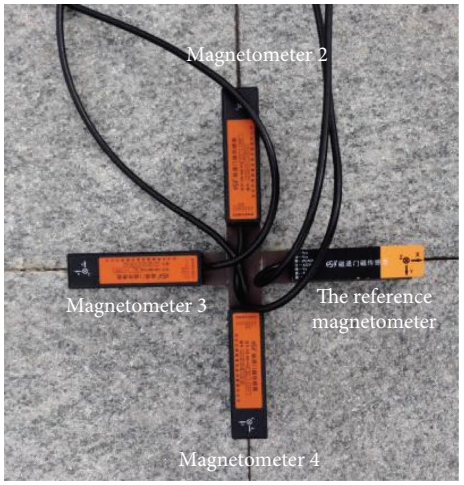

Figure 6: Cross magnetic gradient tensor system.

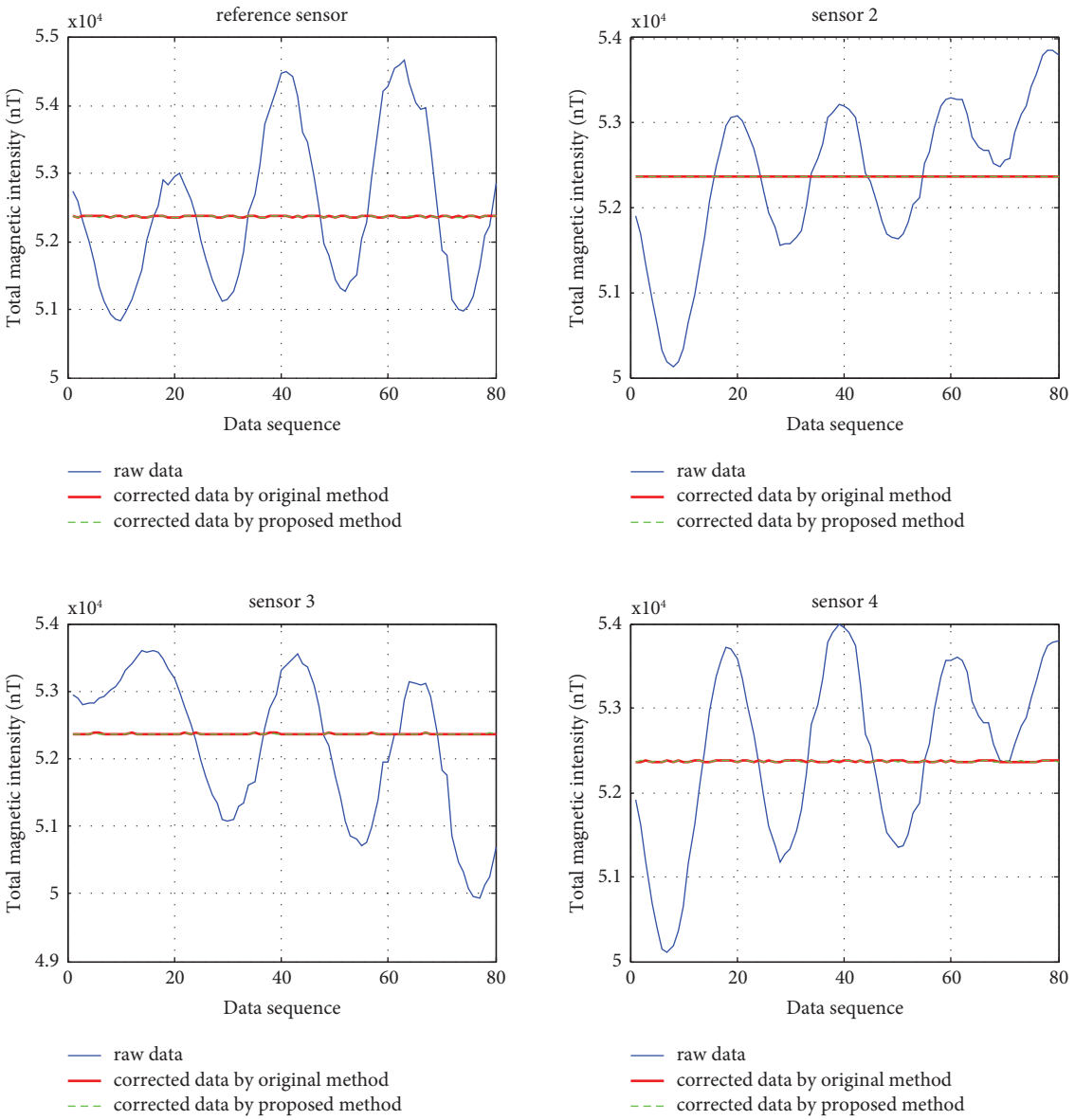

Figure 7: Comparison of total magnetic intensity before and after calibration.

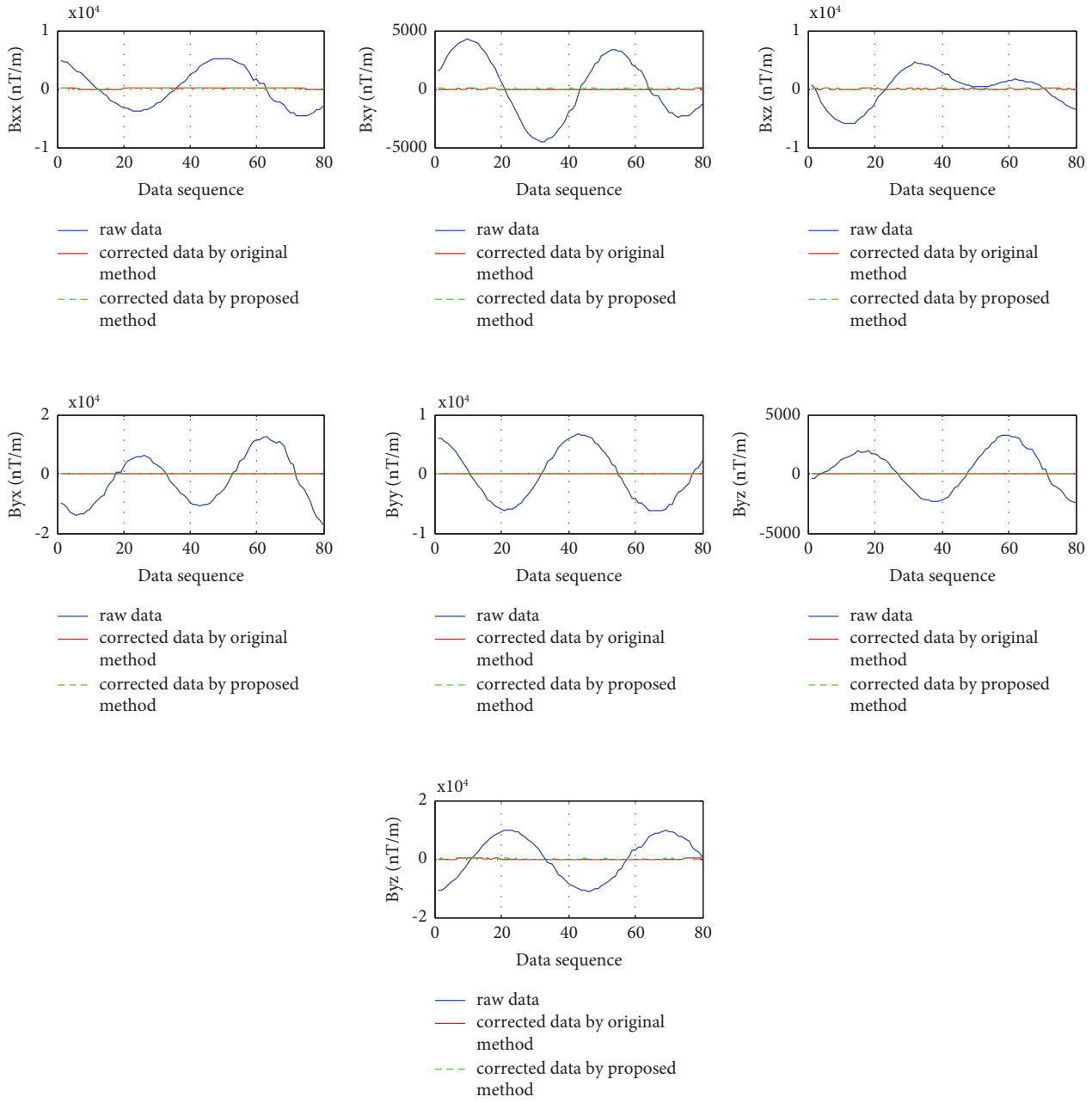

Figure 8: Comparison of tensor components before and after calibration.

Table 5: RMS errors of total magnetic intensity before and after calibration.

	Reference sensor (nT)	Sensor 2 (nT)	Sensor 3 (nT)	Sensor 4 (nT)
Raw data	1147.16	914.77	1080.62	1055.16
Corrected data by the original method	4.199	3.777	4.772	4.725
Corrected data by the proposed method	4.163	3.703	4.654	4.534

Table 6: RMS errors of tensor components before and after calibration.

	B_{xx} (nT/m)	B_{xy} (nT/m)	B_{xz} (nT/m)	B_{yx} (nT/m)	B_{yy} (nT/m)	B_{yz} (nT/m)	B_{zz} (nT/m)
Raw data	3317.25	2723.87	2936.66	8606.44	4405.69	1752.09	7213.74
Corrected data by the original method	51.736	31.316	17.545	29.711	20.691	13.226	65.439
Corrected data by the proposed method	28.302	14.158	17.196	18.655	16.153	13.047	32.214

that the proposed method is more accurate and reliable than the original method.

5. Conclusions

Considering different scale factors, three-axis non-orthogonality, bias, and misalignment errors, the error calibration method of the cross magnetic gradient tensor system is proposed. Firstly, the error calibration model is established, and then, the calibrated parameters are estimated with the total least-squares method. Simulations and experiments with a cross magnetic gradient tensor system are carried out for verification of the proposed error calibration method. The simulation results show that before calibration, the max deviation of the tensor components is 12290 nT/m, and after calibration, the max deviation is reduced to 34.4 nT/m, so the proposed calibration method can calibrate the tensor system effectively. The experiment results show that the RMS errors of the proposed method are smaller than the original method, and the RMSE of B_{xy} can be reduced to 31.316 nT/m by the original method, and however, the RMSE of B_{xy} calibrated by the proposed method is 14.158 nT/m, and 54.79% of errors can be reduced by the proposed method. The proposed method can increase the calibrated accuracy compared with the original least-squares method, so the proposed error calibration method has a high value for practical application. Comparing the two methods, the traditional method (the least-squares method) has much lower accuracy than the proposed method (the total least-squares method). However, the least-squares method has less amount of calculations than the total least-squares method. The singular value decomposition of the matrix is needed in the calculation of the total least-squares method.

In this paper, an error calibration method with the total least-squares method is proposed, and the corrected output by the proposed method is comparatively accurate. However, the magnetic interference of the platform is not considered in this paper, and in the future, an integrated error calibration method should be proposed to calibrate both the magnetic interference and the vector magnetometer errors.

Data Availability

The data supporting the findings of this study are included within the article.

Conflicts of Interest

The authors declare that they have no conflicts of interest.

Acknowledgments

This work research was funded by the National Key Research and Development Program of China (Grant no. 2019YFC1408103).

References

[1] D. A. Clark, "New methods for interpretation of magnetic vector and gradient tensor data I: eigenvector analysis and the normalised source strength," *Exploration Geophysics*, vol. 43, no. 4, pp. 267–282, 2012.

[2] K. M. Lee and M. Li, "Magnetic tensor sensor for gradient-based localization of ferrous object in geomagnetic field," *IEEE Transactions on Magnetics*, vol. 52, no. 8, pp. 1–10, Article ID 4002610, 2016.

[3] J. W. Lv, C. Chi, Z. T. Yu, B. Bo, and S. Qing-Shan, "Research on the asphericity error elimination of the invariant of magnetic gradient tensor," *Acta Physica Sinica*, vol. 64, no. 19, Article ID 190701, 2015.

[4] R. Wiegert, K. Lee, and J. Oeschger, "Improved magnetic STAR methods for real-time, point-by-point localization of unexploded ordnance and buried mines," in *Proceedings of the MTS/IEEE Oceans 2008 Conference*, Quebec City, Canada, September 2008.

[5] Y. H. Pei and H. G. Yeo, "Magnetic gradiometer inversion for underwater magnetic object parameters," in *Proceedings of the OCEANS 2006-Asia Pacific*, pp. 16–19, Singapore, May 2006.

[6] Y. H. Pei and H. G. Yeo, "UXO survey using vector magnetic gradiometer on autonomous underwater vehicle," in *Proceedings of the OCEANS 2009*, pp. 26–29, Biloxi, MS, USA, October 2009.

[7] P. Schmidt, D. A. Clark, K. E. Leslie, M. Bick, D. Tilbrook, and C. Foley, "GETMAG -a SQUID magnetic tensor gradiometer for mineral and oil exploration," *Exploration Geophysics*, vol. 35, no. 4, pp. 297–305, 2004.

[8] Z. G. Song, J. S. Zhang, X. H. Zhang, and X. Xiaoli, "A calibration method of three-Axis magnetometer with noise suppression," *IEEE Transactions on Magnetics*, vol. 50, no. 11, Article ID 4007004, 2014.

[9] Y. Gang, Z. Yingtang, F. Hongbo, R. Guoquan, and L. Zhining, "One-step calibration of magnetic gradient tensor system with nonlinear least square method," *Sensors and Actuators A: Physical*, vol. 229, pp. 77–85, 2015.

[10] H. F. Pang, M. C. Pan, C. B. Wan, C. Jinfei, Z. Xuejun, and L. Feilu, "Integrated compensation of magnetometer array magnetic distortion field and improvement of magnetic object localization," *IEEE Transactions on Geoscience and Remote Sensing*, vol. 52, no. 9, pp. 5670–5676, 2014.

[11] H. U. Auster, K. H. Fornacon, E. Georgescu, K. H. Glassmeier, and U. Motschmann, "Calibration of flux-gate magnetometers using relative motion," *Measurement Science and Technology*, vol. 13, no. 7, pp. 321–1131, 2002.

[12] H. Yu, S. Feng, and W. Li-hua, "Synchronous correction of two three-axis magnetometers using FLANN," *Sensors and Actuators A: Physical*, vol. 179, pp. 312–318, 2012.

[13] Y. Huang and L. H. Wu, "Two-step complete calibration of magnetic vector gradiometer based on functional link artificial neural network and least squares," *IEEE Sensors Journal*, vol. 16, no. 11, pp. 4230–4237, 2016.

[14] Y. Gang, Z. Yingtang, F. Hongbo, Z. Guang, and R. Guoquan, "Linear calibration method of magnetic gradient tensor system," *Measurement*, vol. 56, pp. 8–18, 2014.

[15] Y. Zhen-tao, L. Jun-wei, G. Ning, and Z. Jing, "Error compensation of tetrahedron magnetic gradiometer," *Optics and Precision Engineering*, vol. 22, no. 10, pp. 2683–2690, 2014.

[16] D. A. Clark, "New methods for interpretation of magnetic gradient tensor data," *Aseg Extended Abstracts*, vol. 2012, pp. 1–11, 2012.

[17] L. M. Liu, *Configuration Design, Error Analysis and Underwater Target Detection of Fluxgate Tensor Magnetometer*, Jilin University, Changchun, China, 2012.

[18] C. C. Foster and G. H. Elkaim, "Extension of a two-step calibration methodology to include nonorthogonal sensor axes," *IEEE Transactions on Aerospace and Electronic Systems*, vol. 44, no. 3, pp. 1070–1078, 2008.

[19] C. Chi, J. W. Lv, and J. L. Huang, "Error calibration of cross magnetic gradiometer," *Optics and Precision Engineering*, vol. 25, no. 7, pp. 1919–1926, 2017.

[20] Q. Z. Li, Z. N. Li, Y. T. Zhang, H. B. Fan, and G. Yin, "Two-step linear calibration of planar cross magnetic gradient tensor system," *Chinese Journal of Scientific Instrument*, vol. 38, no. 9, pp. 2232–2242, 2017.

[21] J. L. Zhu, X. Q. Wang, P. L. Wu, Y. M. Bo, and J. Zhang, "Three-dimensional magnetic compass error compensation algorithm based on ellipsoid surface fitting," *Journal of Chinese Inertial Technology*, vol. 20, no. 5, pp. 562–566, 2012.

[22] I. Markovsky and S. Van Huffel, "Overview of total least-squares methods," *Signal Processing*, vol. 87, no. 10, pp. 2283–2302, 2007.

[23] J. F. Vasconcelos, G. Elkaim, C. Silvestre, P. Oliveira, and B. Cardeira, "Geometric approach to strapdown magnetometer calibration in sensor frame," *IEEE Transactions on Aerospace and Electronic Systems*, vol. 47, no. 2, pp. 1293–1306, 2011.